Single-molecule force measurements of the polymerizing dimeric subunit of von Willebrand factor

Sithara S. Wijeratne,[1] Jingqiang Li,[1] Hui-Chun Yeh,[2] Leticia Nolasco,[3] Zhou Zhou,[4] Angela Bergeron,[2] Eric W. Frey,[1] Joel L. Moake,[3] Jing-fei Dong,[4] and Ching-Hwa Kiang[1,3,*]

[1]*Department of Physics and Astronomy, Rice University, Houston, Texas 77005, USA*

[2]*Thrombosis Division, Section of Cardiovascular Sciences, Department of Medicine, Baylor College of Medicine, Houston, Texas 77005, USA*

[3]*Department of Bioengineering, Rice University, Houston, Texas 77005, USA*

[4]*Puget Sound Blood Center and Division of Hematology, Department of Medicine, University of Washington, Seattle, Washington 98104, USA*

(Received 27 May 2015; revised manuscript received 3 December 2015; published 21 January 2016)

Von Willebrand factor (VWF) multimers are large adhesive proteins that are essential to the initiation of hemostatic plugs at sites of vascular injury. The binding of VWF multimers to platelets, as well as VWF proteolysis, is regulated by shear stresses that alter VWF multimeric conformation. We used single molecule manipulation with atomic force microscopy (AFM) to investigate the effect of high fluid shear stress on soluble dimeric and multimeric forms of VWF. VWF dimers are the smallest unit that polymerizes to construct large VWF multimers. The resistance to mechanical unfolding with or without exposure to shear stress was used to evaluate VWF conformational forms. Our data indicate that, unlike recombinant VWF multimers (RVWF), recombinant dimeric VWF (RDVWF) unfolding force is not altered by high shear stress (100 dynes/cm^2 for 3 min at 37°C). We conclude that under the shear conditions used (100 dynes/cm^2 for 3 min at 37°C), VWF dimers do not self-associate into a conformation analogous to that attained by sheared large VWF multimers.

DOI: 10.1103/PhysRevE.93.012410

Von Willebrand factor (VWF) mediates platelet adhesion to exposed subendothelium [1,2]. VWF circulates in blood as multimers with variable masses and adhesive activities (larger multimers are more adhesive). VWF multimers circulating in the plasma can be converted into more adhesive forms by exposure to pathological high levels of fluid shear stress [3]. In contrast, ultralarge forms of VWF multimers (ULVWF) secreted from the Weibel-Palade bodies of endothelial cells, and anchored to the surface of these cells, are intrinsically hyperadhesive and form strong bonds with GP Ib-IX-V complexes on platelets [4,5]. VWF is a multimeric molecule with soluble circulating forms that vary in length (up to 100 μm [5]). During production of VWF multimers, two monomers (each containing propeptides) initially join at their C-termini via disulfide bonds to form a dimer. The dimers (with propeptides eliminated by furin cleavage) then polymerize at their N-termini to form multimers [1–3,6,7]. Each 250-kDa VWF monomeric subunit contains repetitive domains: D′-D3-A1-A2-A3-D4-B1-B2-B3-C1-C2-CK (Fig. 1). The A1 domain binds to the platelet GPIb-IX-V complex; and the A2 domain contains the cleavage site for the VWF-cleaving protease (ADAMTS-13, or a disintegrin and metalloprotease with thrombospondin domains #13). Human ADAMTS-13 cleaves ULVWF multimeric string-like structures following VWF string secretion by, and anchored to, human endothelial cells [5].

Exposure to a pathological level of shear stress induces conformational changes [8,9] and activates soluble VWF multimers by exposing its binding sites for GPIbα. VWF multimers can then mediate the adhesion of platelets. It has been shown that VWF multimers change from a globular to an elongated conformation under shear stress [10–12] and remain in their activated, more adhesive state for hours [13]. Prolonged activation may coincide with the lateral association of VWF multimers into a fibrillar form of VWF [3,8,14].

In this paper, we describe the use of single molecule manipulation by atomic force microscopy (AFM) to monitor the force response of dimeric VWF (DVWF). The data indicate that recombinant (R) DVWF, in contrast to soluble recombinant VWF multimers (RVWF), is not activated by high shear stress.

Recombinant dimeric human VWF (RDVWF) was generated in human embryonic kidney (HEK) 293 cells. cDNA for human VWF, with the propeptide sequence deleted, was inserted into the mammalian expression vector pcDNA3.1 (Life Technologies, Grand Island, NY). The VWF cDNA construct was transfected into 293 cells using the lipid carrier, lipofectamine. Transfected cells were grown first in DMEM medium (Invitrogen, Grand Island, NY) with 5% fetal bovine serum for 48–72 h and then in serum-free DMEM for 24 h. The conditioned medium was collected and RDVWF was purified by affinity chromatography using a polyclonal VWF antibody (DAKO, Carpinteria, CA).

RVWF multimers were produced constitutively from baby hamster kidney (BHK) cells transfected with the cDNA of propepide-containing human VWF monomer. A furin gene was cotransfected into the BHK cells in order to cleave the propeptide portions from the monomers in the VWF dimers, therefore enabling the dimers to polymerize into VWF multimers.

Unreduced 1% SDS-ME agarose (Lonza-Rockland, ME) gel and western blot using rabbit anti-VWF antibody (Ramco Lab-Houston, TX) and secondary goat anti-body linked to horseradish peroxidase (Pierce/Thermo Scientific-Rockford, IL), then chemiluminescence were used to demonstrate the structure difference between the RDVWF (500 kDa) and RVWF multimers (polymerized dimers).

*chkiang@rice.edu

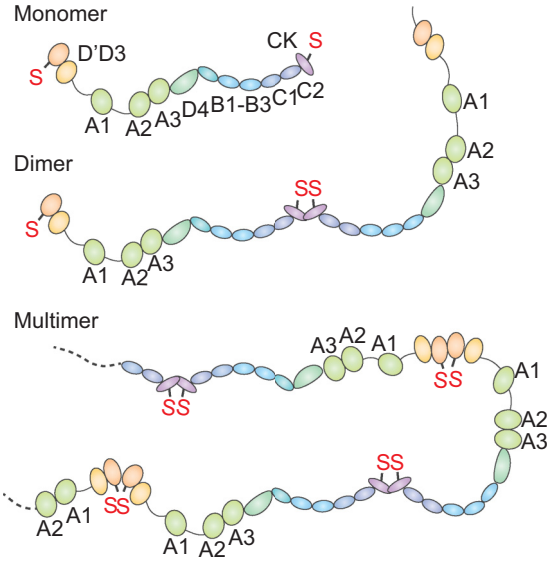

FIG. 1. The domain organization of VWF. RVWF multimers are composed of monomers linked by disulfide bonds (S-S) into multimers. Recombinant DVWFs are composed of two disulfide-linked monomers. Each VWF monomer contains domains that contribute to the function of the VWF multimer. The three A domains (A1, A2, A3) contain the platelet GPIb-binding site (domain A1), the cleavage site for ADAMTS-13 (domain A2), and a collagen-binding site (domain A3).

Ellman's reagent 5,5-dithiobis-(2 nitrobenzoic acid) or DNTB (Sigma Aldrich, St. Louis, MO) was used to quantify free thiol groups in similar concentrations of VWF antigen (170 ± 50 ng/ml) in the samples of recombinant dimers or multimers. Free thiols were quantified by comparison with cysteine (Sigma Aldrich, St. Louis, MO) in a range concentration (0.13–1.50 mM) ($n = 7$).

RDVWF (500 μl at 170 ± 40 ng/ml) was exposed to 100 dynes/cm^2 shear stress for 3 min at 37°C on a cone-and-plate viscometer (RS1, HAAKE Instrument Inc., Paramus, NJ), as previously described [15] [Figs. 2(c) and 4]. The surfaces of the cone and plate were coated with 5% bovine serum albumin (BSA) for 15 min to 4 h at room temperature and rinsed gently with deinoized water before experiments. Shear stress was calculated based on a constant shear rate of 10 000 s^{-1} and a viscosity of 1 cp for RDVWFs in suspension. RDVWF was subjected to AFM experiments within 1 h after exposure to shear stress, and the results were compared to RVWF multimers [Fig. 4(e)]. Time-dependent experiments were conducted for a period of 12 h after shear exposure, with each individual time experiment lasting for 2 h. Free thiol measurements by Ellman's assay were performed on the same set of pre- and postshear RDVWF and RVWF multimers [Figs. 2(b) and 2(c)].

In addition to the disulfide bonds that link VWF monomers into VWF multimers, the large VWF multimers have exposed free thiols [3]. These exposed thiols may enable the large multimers to form mixed disulfide bonds and associate laterally into even larger fibrillar forms [3]. This is likely to occur when they are forced into close multimer-multimer contact by shear stress. In contrast, RDVWF have few free thiols to promote the

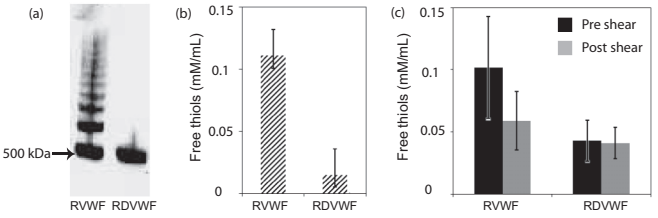

FIG. 2. Free thiols in RDVWF and RVWF multimer. (a) Unreduced 1% ME agarose gel and western blot using rabbit anti-VWF antibody plus secondary goat antirabbit antibody linked to horseradish peroxidase demons- trating the structural difference between the rdimer (500kD) and RVWF multimers (polymerized dimers). (b) Ellman's reagent 5,5-dithiobis-(2nitrobenzoic acid), or DTNB was used to quantify free thiol groups in equivalent quantities of VWF antigen RDVWF (170 ± 60 ng/ml) and RVWF multimers (170 ± 70 ng/ml). Free thiols were quantified by comparison with a range of cysteine concentrations (Number of experiments, $n = 7$). (c) Free thiol groups were also quantified in the samples of recombinant dimers or multimers in conditioned media (supernatant of transfected BHK cells) with similar VWF antigen levels (170 ± 40 ng/ml) before and after shear at 100 dynes/cm^2 for 3 min at a constant temperature of 37 °C. Free thiols were quantified as in (b) and (c), by comparison with a standard sulfhydryl (cysteine in a range concentrations (0.13–1.50 mM) ($n = 7$). Identical samples were used for AFM studies.

lateral association of VWF dimers under shear. The difference between exposed free thiols in RDVWF and RVWF multimers before and after exposure to 100 dynes/cm^2 fluid shear stress is demonstrated in Fig. 2(c).

For stretching experiments, RDVWF molecules were equilibrated at 37°C prior to depositing onto a fresh gold-coated substrate at room temperature for 10–15 min. The AFM tip was brought in contact with the surface for 1–3 s in order to establish a contact between the RDVWF molecules under study and the cantilever tip, as depicted schematically in Fig. 3(a). All of the force measurements were taken in aqueous phosphate-buffered saline (PBS, pH 7.4) with a pulling velocity of 1000 nm/s. The force versus time data were converted to force versus change in molecular end-to-end extension curves. Unfolding peaks in the force curves were fitted with the wormlike chain (WLC) model [Figs. 3(b) and 3(c)] [16–19], as follows:

$$F(x) = \frac{\beta}{L_p}\left[\frac{1}{4(1-\frac{x}{L_c})^2} - \frac{1}{4} + \frac{x}{L_c}\right], \qquad (1)$$

where x is the extension, F is the force, and $\beta = 1/k_B T$, where k_B is the Boltzmann constant, T is the temperature, and L_p and L_c are the persistence length and contour length. Histograms of the force peaks were compiled and distributions were fitted to a Gaussian curve [Fig. 3(d)]. The peaks of these Gaussian curves represent the most probable values. Time-dependent experiments were conducted within a period of 12 h following the shear exposure, as shown in Fig. 4.

Figure 3(b) shows representative force-extension curves corresponding to the mechanical unfolding of RDVWF by AFM. Because the AFM tip could pick up any domain in the samples, the number of peaks within each force curve was

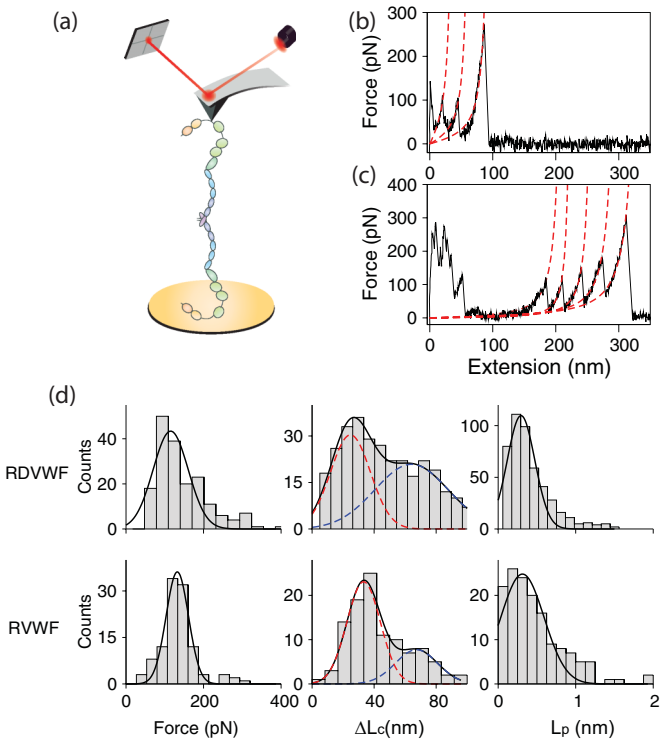

FIG. 3. AFM unfolding of RDVWF and RVWF multimer. (a) Illustration of an AFM pulling experiment on RDVWF. Force-extension experiments on (b) RDVWF and (c) RVWF. The force curves are fit to the wormlike chain model (dashed lines) of polymer elasticity in order to determine the change in contour length, ΔL_c [Eq. (1)]. (d) Top: AFM unfolding of RDVWF. The histogram shows a peak at 120 pN. The solid line indicates the fitted Gaussian curve. Histogram of the ΔL_c shows a major peak at 25 nm (red dotted line) and a minor peak at 65 nm (blue dotted line) from fitting to double Gaussian curves. Histogram of the persistence length, L_p, shows a peak at 0.3 nm. Bottom: AFM unfolding of RVWF. The histograms show an unfolding force of 130 pN, $\Delta L_c =$ 32 and 67 nm, and $L_p = 0.3$ nm. The data points in each of the experiments for RDVWF and RVWF unfolding force, ΔL_c and L_p histograms range between 100 and 500.

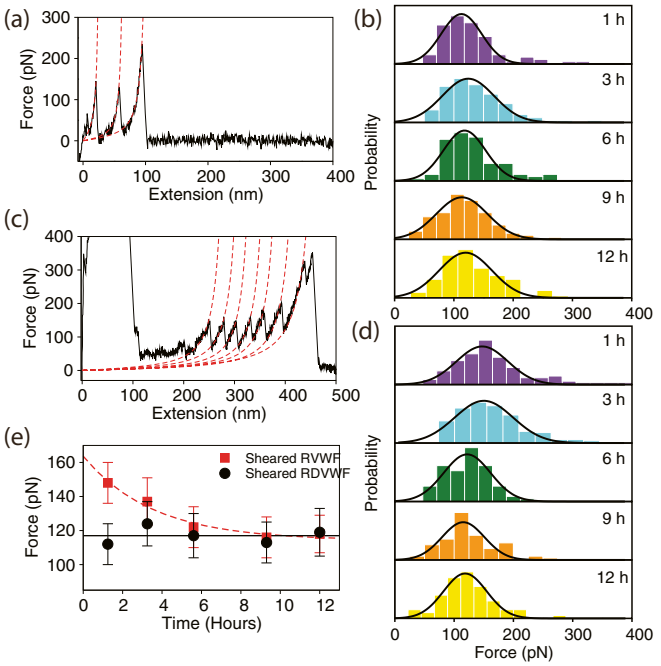

FIG. 4. Sheared RDVWF and RVWF multimer time-dependent force data. (a) Representative force-extension curve of sheared RDVWF. (b) The unfolding force distributions of RDVWF as a function of time after exposure to shear stress. The solid lines indicate the fitted Gaussian curves. (c) Representative force-extension curve of sheared RVWF multimer. (d) The unfolding force distributions of RVWF multimer as a function of time after exposure to shear stress. The solid lines indicate the fitted Gaussian curves. (e) The sheared RDVWF unfolding force does not change appreciably with time after shear exposure. The solid line is a linear fit to the data (solid circles) with an average force of 120 pN. The dashed line is a fit to an exponential curve, $F(t) = F_p + (F_s - F_p)\exp(-t/\tau)$ of RVWF multimer unfolding force (solid squares). The error bars are half of the bin width of the histograms in (b) and (d). The number of data points in sheared RDVWF unfolding force histograms range between 70 to 200.

randomly distributed. The force-extension curve of RDVWF was qualitatively similar to the RVWF multimer, except for the number of unfolding peaks. The force curves were fitted with a WLC model of polymer elasticity. Figure 3(d) shows the histogram of the unfolding force of the RDVWF (120 pN) at a pulling speed of 1000 nm/s. The histogram of the change in contour length, ΔL_c, fitted with double Gaussian distributions, had major peaks at 25 and 65 nm [Fig. 3(d)]. These values correspond to the length of unfolded protein domains of 60 and 190 amino acids (aa), respectively, assuming 0.36 nm per residue [13,20,21]. The persistence length, L_p, of the RDVWF was 0.3 nm [Fig. 3(d)]. The unfolding force, ΔL_c, and L_p distributions are consistent with protein domain unfolding. This is supported by: (i) at 1000 nm/s pulling velocity, the unfolding force varies between 100–130 pN [13], (ii) the increase in the contour length for each added peak ΔL_c is 25 nm, consistent with the contour length of an unfolded full or partial VWF domain [13]; and (iii) the persistence length, L_p, of 0.3 nm is consistent with an unfolded protein [13,20,22–26]. The uncertainty in the unfolding force, ΔL_c and L_p are 20 pN, 5 nm and 0.1 nm, respectively.

The values associated with RDVWF unfolding force are similar to the measured unfolding force of the RVWF multimer [$F = 130$ pN, $\Delta L_c = 32$ and 67 nm, $L_p = 0.3$ nm, Fig. 3(d)]. Force-extension curves demonstrate that the VWF domains unfold in a sequential manner, producing one to four peaks for RDVWF [Fig. 3(b)]. This is consistent with one to two unfolding peaks per VWF monomer in a DVWF [13]. RVWF multimers had more unfolding force peaks in the force-extension curves [Fig. 3(c)] than RDVWF, compatible with the stretching of single molecules containing a larger number of repeating VWF monomeric subunits (and unfolding domains) [13].

Peak unfolding force measurements of RDVWF were made at different times after exposure to high shear stress. Figure 4 shows that the sheared RDVWF unfolding force showed no significant change over time, compared to the initial measurements (0.5 h). Fitting the data to a straight line yields a force of 120 pN, which agrees with the unfolding force

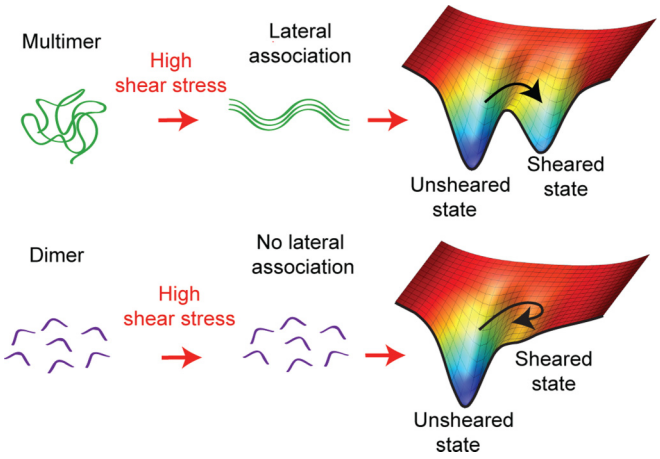

FIG. 5. A model of shear-induced conformational changes in VWF. Shear stress results in the lateral association of RVWF multimers, but not RDVWF into fibrils. This can be explained by that, in the VWF multimer, high shear stress switches VWF to an intermediate state (solid arrows), which has a different unfolding force. However, for the RDVWF, a metastable intermediate state is lacking. The metastable state in RVWF has a shift in force distribution.

of RDVWF that was not subjected to shear. In contrast, the peak unfolding force of RVWF multimers decreased over time, reaching equilibrium with a half-life of 3.5 h. The exponential equation $F(t) = F_p + (F_s - F_p)\exp(-t/\tau)$ was used to fit the data, where F_s indicates the peak force of RVWF multimers immediately after the shear, F_p is the equilibrium force, and τ is the time constant, yielding $F_s = 164$ pN, $F_p = 115$ pN, and $\tau = 3.5$ h. This result indicates that shear-induced conformational alterations of RVWF subsequently return slowly from an active to inactive state after the cessation of high shear stress.

The unfolding force peaks of RDVWF were similar to that of RVWF multimers. The A2 domain, with 177 residues lacking disulfide bonds, may unfold in response to an applied force of about 120 pN. This is not a sufficient force to unfold VWF A1 and A3 domains that contain disulfide bonds. Upon exposure to a pathological level of shear stress, the RVWF unfolding force shifts to a higher value [13]. However, the RDVWF unfolding force remains unchanged. This may be explained by the induction under high shear stress of the lateral association of RVWF multimers, but not RDVWF, into fibrils [3]. For RVWF multimers, this process may contribute to lateral multimer-multimer interactions (probably via free thiols in RVWF multimers) and the associated conformational changes in A1 domains that enhance the capacity of sheared RVWF multimers to adhere to platelet GPIb-IX-V receptors.

RVWF multimers can be activated by shear stress and trapped in activated states for several hours, whereas RDVWF cannot [3]. These findings suggest that the higher order of intermolecular and interdomain organization is responsible for the activation of RVWF multimers into a more platelet-adhesive state (Fig. 5). The slow relaxation of sheared RVWF multimers indicates that a significant free-energy barrier exists between shear-activated and nonactivated A1 domains in the monomeric subunits of RVWF multimers. In contrast, RDVWF has a relatively small mass and little or no shear-induced RDVWF-RDVWF interaction. RDVWF forms possess a large entropy, and therefore lack a stable intermolecular "packed" state without a kinetic barrier to association-dissociation. These observations emphasize the importance of the RVWF multimeric structure in mechanical activation during hemostasis.

In summary, we compared the force-induced domain unfolding of RDVWF with RVWF multimers. In contrast to RVWF multimers, the peak unfolding force of RDVWF subjected to 100 dynes/cm^2 shear force did not change compared to unsheared RDVWF. This was probably because this 100 dynes/cm^2 shear stress does not induce RVWF dimers (with few free thiols) to associate into fibrils (as do RVWF multimers with more free thiols). In contrast to sheared RVWF multimers, sheared RDVWF remains in its native conformational state that is less adherent to platelets than sheared RVWF multimers [27].

ACKNOWLEDGMENTS

This work was supported by National Science Foundation (Grant No. 0907676), the Welch Foundation (Grant No. C-1632), the Keck Center Nanobiology Interdisciplinary Graduate Training Program of the Gulf Coast Consortia (National Institutes of Health, Grant No. T32EB009379), the Hammill Foundation, the Mary R. Gibson Foundation, and the Mabel and Everett Hinkson Memorial Fund at Rice University.

[1] Z. M. Ruggeri, J. Thromb. Haemost. **1**, 1335 (2003).
[2] J. E. Sadler, Annu. Rev. Biochem. **67**, 395 (1998).
[3] H. Choi, K. Aboulfatova, H. J. Pownall, R. Cook, and J.-F. Dong, J. Biol. Chem. **282**, 35604 (2007).
[4] J. L. Moake, N. A. Turner, N. A. Stathopoulos, L. H. Nolasco, and J. D. Hellums, J. Clin. Invest. **78**, 1456 (1986).
[5] M. Arya, B. Anvari, G. M. Romo, M. A. Cruz, J.-F. Dong, L. V. McIntire, J. L. Moake, and J. A. Lopez, Blood **99**, 3971 (2002).
[6] J. L. Moake, C. K. Rudy, J. H. Troll, M. J. Weinstein, N. M. Colannino, J. Azocar, R. H. Seder, S. L. Hong, and D. Deykin, N. Engl. J. Med. **307**, 1432 (1982).
[7] J. Kim, C.-Z. Zhang, X. Zhang, and T. A. Springer, Nature **466**, 992 (2010).
[8] H.-C. Yeh, Z. Zhou, H. Choi, S. Tekeoglu, W. May III, C. Wang, N. Turner, F. Scheiflinger, J. L. Moake, and J.-F. Dong, J. Thromb. Haemost. **8**, 2778 (2010).
[9] S. Lippok, T. Obser, J. P. Muller, V. K. Stierle, M. Benoit, U. Budde, R. Schneppenheim, and J. O. Radler, Biophys. J. **105**, 1208 (2013).
[10] C. A. Siediecki, B. J. Lestini, K. K. Kottke-Marchant, S. J. Eppell, D. L. Wilson, and R. E. Marchant, Blood **88**, 2939 (1996).

[11] S. W. Schneider, S. Nuschele, A. Wixforth, C. Gorzelanny, A. Alexander-Katz, R. R. Netz, and M. F. Schneider, Proc. Natl. Acad. Sci. USA **104**, 7899 (2007).
[12] I. Singh, E. Themistou, L. Porcar, and S. Neelamegham, Biophys. J. **96**, 2313 (2009).
[13] S. S. Wijeratne, E. Botello, H.-C. Yeh, Z. Zhou, A. L. Bergeron, E. W. Frey, J. M. Patel, L. Nolasco, N. A. Turner, J. L. Moake, *et al.*, Phys. Rev. Lett. **110**, 108102 (2013).
[14] J.-F. Dong, J. L. Moake, L. Nolasco, A. Bernardo, W. Arceneaux, C. N. Shrimpton, A. J. Schade, L. V. McIntire, K. Fujikawa, and J. A. López, Blood **100**, 4033 (2002).
[15] J. N. Zhang, A. L. Bergeron, Q. Yu, C. Sun, L. V. McIntire, J. A. López, and J. F. Dong, Thromb. Haemost. **88**, 817 (2002).
[16] C. Bustamante, J. F. Marko, E. D. Siggia, and S. Smith, Science **265**, 1599 (1994).
[17] O. B. Bakajin, T. A. J. Duke, C. F. Chou, S. S. Chan, R. H. Austin, and E. C. Cox, Phys. Rev. Lett. **80**, 2737 (1998).
[18] B. Onoa, S. Dumont, J. Liphardt, S. B. Smith, I. Tinoco Jr., and C. Bustamante, Science **299**, 1892 (2003).
[19] W.-S. Chen, W.-H. Chen, Z. Chen, A. A. Gooding, K.-J. Lin, and C.-H. Kiang, Phys. Rev. Lett. **105**, 218104 (2010).
[20] X. Zhang, K. Halvorsen, C.-Z. Zhang, W. P. Wong, and T. A. Springer, Science **324**, 1330 (2009).
[21] F. Oesterhelt, D. Oesterhelt, M. Pfeiffer, A. Engel, H. E. Gaub, and D. J. Müller, Science **288**, 143 (2000).
[22] M. Rief, F. Oesterhelt, B. Heymann, and H. E. Gaub, Science **275**, 1295 (1997).
[23] M. Carrion-Vazquez, A. F. Oberhauser, S. B. Fowler, P. E. Marszalek, S. E. Broedel, J. Clarke, and J. M. Fernandez, Proc. Natl. Acad. Sci. USA **96**, 3694 (1999).
[24] P. E. Marszalek, H. Lu, H. Li, M. Carrion-Vazquez, A. F. Oberhauser, K. Schulten, and J. M. Fernandez, Nature **402**, 100 (1999).
[25] N. C. Harris, Y. Song, and C.-H. Kiang, Phys. Rev. Lett. **99**, 068101 (2007).
[26] E. Botello, N. C. Harris, J. Sargent, W.-H. Chen, K.-J. Lin, and C.-H. Kiang, J. Phys. Chem. B **113**, 10845 (2009).
[27] E. Themistou, I. Singh, C. W. Shang, S. V. Balu-Iyer, P. Alexandridis, and S. Neelamegham, Biophys. J. **97**, 2567 (2009).